第 48 卷 第 3 期/2021 年 2 月/中国激光 研究论文

中国激光

原子介质中的近共振增益光栅

董雅宾[1,2*]，庞嘉璐[1]，杨丽[1]，刘瑶瑶[1]

[1]山西大学物理电子工程学院，山西 太原 030006；

[2]山西大学极端光学协同创新中心，山西 太原 030006

摘要 研究了一种 N 型四能级原子结构中的近共振增益光栅(NRGG)效应。结果表明，当耦合场的失谐值为 0，探测场和调制场的失谐值接近于 0 时，利用调制场和耦合场可以调控探测场的增益和相位，使得探测场的能量和高阶衍射效率都得到显著提高。在这个过程中，调制场强度存在阈值。获得了具有增益高、衍射能力强和阈值可控的光栅，该光栅在全光开关、全光逻辑门和全光调制等应用中将会发挥较大的作用。

关键词 量子光学；电磁感应光栅；光增益；衍射效率

中图分类号 O431.2 **文献标志码** A **doi**：10.3788/CJL202148.0312002

1 引 言

原子中的量子相干效应产生了许多有趣的现象，其中电磁感应透明[1](EIT)为深入研究光与原子的相互作用开辟了新的途径。基于 EIT 的原子相干效应如无粒子数反转激光[2-4]、非线性量子光学[5-7]和简并能级的 EIT 现象[8-9]等引起了学者们的广泛关注。此外，EIT 还被应用于光存储[10-11]和单光子开关[12-13]等各种量子器件中。在 Λ 型三能级原子 EIT 系统中，用驻波代替耦合场的行波以形成电磁感应光栅[14](EIG)。EIG 得到了广泛关注和研究[15-18]，学者们分别在冷原子[19]和热原子[20]的实验中证明了 EIG 现象。另外，学者们还提出了许多基于 EIG 的应用，如全光开关[21-23]、相干诱导光子带隙[24]和静止光脉冲[25-26]等。

与传统光栅相比，EIG 可以主动实时调控光场，能够同时实现振幅和相位的调制。然而，EIG 获得的衍射效率相对较小。为了提高衍射效率，de Araujo[27]提出了一种电磁感应相位光栅(EIPG)，其一阶衍射效率接近理想正弦相位光栅。之后，许多研究者对 EIPG 进行了深入的研究[28-29]。尽管如此，EIPG 的高阶衍射效率还是相对较小，探测场的能量并没有得到很好的放大。本文从理论上研究了一种 N 型四能级原子介质中的近共振增益光栅(NRGG)效应。在调制场和耦合场的共同作用下，得到了具有增益高、衍射能力强和阈值可控的光栅。此外，还具体研究了影响衍射效率的相关因素。

2 模型与方程

图 1(a)是 N 型四能级原子系统的能级结构示意图，与原子系统作用的三束光分别为探测场、耦合场和调制场，其中，Ω_p、Ω_c 和 Ω_m 分别为探测场、耦合场和调制场的半拉比频率。探测场和驻波耦合场分别驱动跃迁$|1\rangle\leftrightarrow|3\rangle$和$|2\rangle\leftrightarrow|3\rangle$。调制场作用于基态能级$|1\rangle$和激发态能级$|4\rangle$。能级跃迁$|4\rangle\leftrightarrow|3\rangle$和$|2\rangle\leftrightarrow|1\rangle$为偶极禁戒。如图 1(b)所示，探测场的传播方向沿着 z 轴方向，耦合场在原子区域叠加并在 x 方向形成驻波场，可以表示为 $\Omega_c=\Omega\sin(\pi x/\Lambda)$，其中，$\Omega$ 为耦合场的半拉比频率的最大值，Λ 为驻波空间周期，x 为驻波在 x 方向上的坐标。

在旋波近似下，给出了四能级原子系统的密度矩阵演化方程

收稿日期：2020-08-18；**修回日期**：2020-09-16；**录用日期**：2020-09-27

基金项目：国家自然科学基金(11004126，61275212)

*E-mail：ybdong@sxu.edu.cn

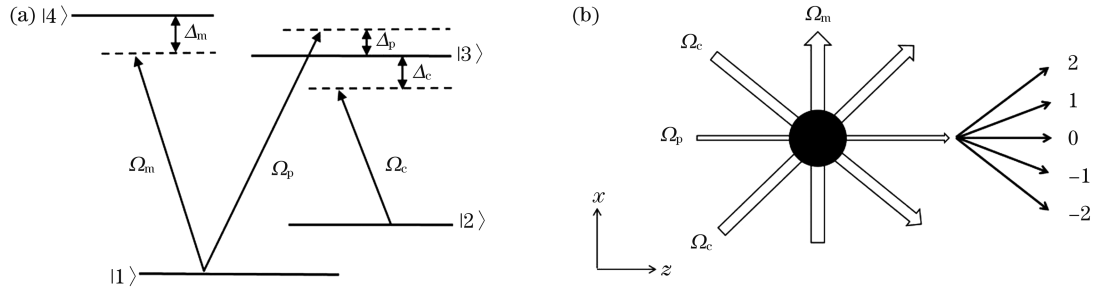

图 1 原子系统的能级结构及场与原子系统间的位置关系。(a) N 型四能级原子系统的能级结构;(b)探测场、耦合场和调制场与原子系统的位置关系,零阶、一阶和二阶衍射方向标于图中

Fig. 1 Energy level structure of atomic system and position relation between fields and atomic system. (a) Four-level N-type atomic system; (b) spatial configuration of probe, modulation, and coupling fields with respect to atomic sample in which zeroth-order, first-order and second-order diffraction directions are indicated

$$\frac{\partial\rho_{11}}{\partial t}=\Gamma_{41}\rho_{44}+\Gamma_{31}\rho_{33}+\Gamma_{21}\rho_{22}+\mathrm{i}(\rho_{31}\Omega_{\mathrm{p}}^{*}-\rho_{13}\Omega_{\mathrm{p}})+\mathrm{i}(\rho_{41}\Omega_{\mathrm{m}}^{*}-\rho_{14}\Omega_{\mathrm{m}}),\tag{1}$$

$$\frac{\partial\rho_{22}}{\partial t}=\Gamma_{42}\rho_{44}+\Gamma_{32}\rho_{33}-\Gamma_{21}\rho_{22}+\mathrm{i}(\rho_{32}\Omega_{\mathrm{c}}^{*}-\rho_{23}\Omega_{\mathrm{c}}),\tag{2}$$

$$\frac{\partial\rho_{33}}{\partial t}=\Gamma_{43}\rho_{44}-\Gamma_{32}\rho_{33}-\Gamma_{31}\rho_{33}+\mathrm{i}(\rho_{23}\Omega_{\mathrm{c}}-\rho_{32}\Omega_{\mathrm{c}}^{*})+\mathrm{i}(\rho_{13}\Omega_{\mathrm{p}}-\rho_{31}\Omega_{\mathrm{p}}^{*}),\tag{3}$$

$$\frac{\partial\rho_{44}}{\partial t}=-(\Gamma_{43}+\Gamma_{42}+\Gamma_{41})\rho_{44}+\mathrm{i}(\rho_{14}\Omega_{\mathrm{m}}-\rho_{41}\Omega_{\mathrm{m}}^{*}),\tag{4}$$

$$\frac{\partial\rho_{21}}{\partial t}=-\gamma'_{21}\rho_{21}+\mathrm{i}\rho_{31}\Omega_{\mathrm{c}}^{*}-\mathrm{i}\rho_{24}\Omega_{\mathrm{m}}-\mathrm{i}\rho_{23}\Omega_{\mathrm{p}},\tag{5}$$

$$\frac{\partial\rho_{31}}{\partial t}=-\gamma'_{31}\rho_{31}+\mathrm{i}\rho_{21}\Omega_{\mathrm{c}}-\mathrm{i}\rho_{34}\Omega_{\mathrm{m}}+\mathrm{i}(\rho_{11}-\rho_{33})\Omega_{\mathrm{p}},\tag{6}$$

$$\frac{\partial\rho_{41}}{\partial t}=-\gamma'_{41}\rho_{41}-\mathrm{i}\rho_{43}\Omega_{\mathrm{p}}+\mathrm{i}(\rho_{11}-\rho_{44})\Omega_{\mathrm{m}},\tag{7}$$

$$\frac{\partial\rho_{23}}{\partial t}=-\gamma'_{23}\rho_{23}-\mathrm{i}(\rho_{22}-\rho_{33})\Omega_{\mathrm{c}}^{*}-\mathrm{i}\rho_{21}\Omega_{\mathrm{p}}^{*},\tag{8}$$

$$\frac{\partial\rho_{42}}{\partial t}=-\gamma'_{42}\rho_{42}-\mathrm{i}\rho_{43}\Omega_{\mathrm{c}}+\mathrm{i}\rho_{12}\Omega_{\mathrm{m}},\tag{9}$$

$$\frac{\partial\rho_{43}}{\partial t}=-\gamma'_{43}\rho_{43}+\mathrm{i}\rho_{13}\Omega_{\mathrm{m}}-\mathrm{i}\rho_{42}\Omega_{\mathrm{c}}^{*}-\mathrm{i}\rho_{41}\Omega_{\mathrm{p}}^{*},\tag{10}$$

式中:$\gamma'_{21}=\gamma_{21}-\mathrm{i}(\Delta_{\mathrm{p}}-\Delta_{\mathrm{c}})$,$\gamma'_{31}=\gamma_{31}-\mathrm{i}\Delta_{\mathrm{p}}$,$\gamma'_{41}=\gamma_{41}-\mathrm{i}\Delta_{\mathrm{m}}$,$\gamma'_{23}=\gamma_{23}+\mathrm{i}\Delta_{\mathrm{c}}$,$\gamma'_{42}=\gamma_{42}-\mathrm{i}(\Delta_{\mathrm{c}}+\Delta_{\mathrm{m}}-\Delta_{\mathrm{p}})$,$\gamma'_{43}=\gamma_{43}-\mathrm{i}(\Delta_{\mathrm{m}}-\Delta_{\mathrm{p}})$;$\gamma_{ij}$ 为能级 i 到 j 的相位衰减,$\gamma_{ij}=(\Gamma_i+\Gamma_j)/2$,其中 Γ_i 为 i 能级的衰减项,Γ_j 为 j 能级的衰减项;Γ_{ij} 为对应能级间的粒子数衰减率;Δ_{m},Δ_{c},Δ_{p} 分别为调制场、耦合场和探测场的频率失谐量,$\Delta_{\mathrm{m}}=\omega_{\mathrm{m}}-\omega_{41}$,$\Delta_{\mathrm{c}}=\omega_{\mathrm{c}}-\omega_{32}$,$\Delta_{\mathrm{p}}=\omega_{\mathrm{p}}-\omega_{31}$,其中 ω_{m},ω_{c} 和 ω_{p} 为圆频率,ω_{41}、ω_{32} 和 ω_{31} 为相应的原子跃迁频率;$\Omega_{\mathrm{m}}=\mu_{41}E_{\mathrm{m}}/(2\hbar)$,$\Omega_{\mathrm{c}}=\Omega\sin(\pi x/\Lambda)$,$\Omega_{\mathrm{p}}=\mu_{31}E_{\mathrm{p}}/2\hbar$,其中 $\Omega=\mu_{32}E_{\mathrm{c}}\div(2\hbar)$,$\mu_{41}$,$\mu_{32}$,$\mu_{31}$ 分别为对应的偶极矩,E_{m},E_{c},E_{p} 分别为调制场、耦合场和探测场的电场强度,$\hbar$ 为约化普朗克常量;* 表示复共轭;t 为时间;ρ_{ij} 为密度矩阵元且 $\rho_{ij}=\rho_{ji}^{*}$。闭合原子系统需要满足且 $\rho_{11}+\rho_{22}+\rho_{33}+\rho_{44}=1$。

稳态下,通过计算得到

$$\frac{\rho_{31}}{\Omega_{\mathrm{p}}}=\{(|\Omega_{\mathrm{m}}|^{2}-|\Omega_{\mathrm{c}}|^{2}+\gamma'_{21}\gamma'_{24})\Omega_{\mathrm{m}}\rho_{14}^{(0)}+(|\Omega_{\mathrm{c}}|^{2}-|\Omega_{\mathrm{m}}|^{2}+\gamma'_{34}\gamma'_{24})\Omega_{\mathrm{c}}\rho_{23}^{(0)}+\mathrm{i}(\gamma'_{34}|\Omega_{\mathrm{m}}|^{2}+\gamma'_{21}|\Omega_{\mathrm{c}}|^{2}+\gamma'_{21}\gamma'_{24}\gamma'_{34})(\rho_{11}^{(0)}-\rho_{33}^{(0)})\}\div\{(|\Omega_{\mathrm{m}}|^{2}-|\Omega_{\mathrm{c}}|^{2}-\gamma'_{31}\gamma'_{21})(|\Omega_{\mathrm{m}}|^{2}-|\Omega_{\mathrm{c}}|^{2}-\gamma'_{34}\gamma'_{24})+|\Omega_{\mathrm{m}}|^{2}(\gamma'_{31}+\gamma'_{24})(\gamma'_{21}+\gamma'_{34})\},\tag{11}$$

式中：

$$\rho_{11}^{(0)}=\{|\Omega_c|^2(\gamma'_{23}+\gamma'_{32})\Gamma_{31}[(\Gamma_{41}+\Gamma_{42})\gamma'_{14}\gamma'_{41}+|\Omega_m|^2(\gamma'_{14}+\gamma'_{41})]\}\div$$
$$\{|\Omega_m|^2(\gamma'_{14}+\gamma'_{41})[\gamma'_{23}\Gamma_{31}(3|\Omega_c|^2+\Gamma_{42}\gamma'_{32})+4|\Omega_c|^2\gamma'_{32}\Gamma_{31}+\Gamma_{42}\gamma'_{23}(|\Omega_c|^2+\Gamma_{32}\gamma'_{32})]+$$
$$(\Gamma_{41}+\Gamma_{42})(\gamma'_{23}+\gamma'_{32})\gamma'_{14}\gamma'_{41}|\Omega_c|^2\Gamma_{31}\}, \tag{12}$$

$$\rho_{14}^{(0)}=[-\mathrm{i}|\Omega_c|^2\Omega_m(\gamma'_{23}+\gamma'_{32})\Gamma_{31}(\Gamma_{41}+\Gamma_{42})\gamma'_{41}]\div$$
$$\{|\Omega_m|^2(\gamma'_{14}+\gamma'_{41})[\gamma'_{23}\Gamma_{31}(3|\Omega_c|^2+\Gamma_{42}\gamma'_{32})+4|\Omega_c|^2\gamma'_{32}\Gamma_{31}+\Gamma_{42}\gamma'_{23}(|\Omega_c|^2+\Gamma_{32}\gamma'_{32})]+$$
$$(\Gamma_{41}+\Gamma_{42})(\gamma'_{23}+\gamma'_{32})\gamma'_{14}\gamma'_{41}|\Omega_c|^2\Gamma_{31}\}, \tag{13}$$

$$\rho_{23}^{(0)}=\{-\mathrm{i}\Omega_c^*|\Omega_m|^2(\gamma'_{14}+\gamma'_{41})[|\Omega_c|^2(\Gamma_{31}-\Gamma_{42})+(\Gamma_{31}+\Gamma_{32})\Gamma_{42}\gamma'_{32}]\}\div$$
$$\{|\Omega_m|^2(\gamma'_{14}+\gamma'_{41})[\gamma'_{32}\Gamma_{31}(3|\Omega_c|^2+\Gamma_{42}\gamma'_{23})+4|\Omega_c|^2\gamma'_{23}\Gamma_{31}+\Gamma_{42}\gamma'_{32}(|\Omega_c|^2+\Gamma_{32}\gamma'_{23})]+$$
$$(\Gamma_{41}+\Gamma_{42})(\gamma'_{23}+\gamma'_{32})\gamma'_{14}\gamma'_{41}|\Omega_c|^2\Gamma_{31}\}, \tag{14}$$

$$\rho_{33}^{(0)}=[|\Omega_c|^2|\Omega_m|^2(\gamma'_{23}+\gamma'_{32})(\gamma'_{14}+\gamma'_{41})\Gamma_{42}]\div$$
$$\{|\Omega_m|^2(\gamma'_{14}+\gamma'_{41})[\gamma'_{23}\Gamma_{31}(3|\Omega_c|^2+\Gamma_{42}\gamma'_{32})+4|\Omega_c|^2\gamma'_{32}\Gamma_{31}+\Gamma_{42}\gamma'_{23}(|\Omega_c|^2+\Gamma_{32}\gamma'_{32})]+$$
$$(\Gamma_{41}+\Gamma_{42})(\gamma'_{23}+\gamma'_{32})\gamma'_{14}\gamma'_{41}|\Omega_c|^2\Gamma_{31}\}。 \tag{15}$$

由探测场引起的介质的慢变极化强度为

$$P_p=\varepsilon_0\chi_pE_p=N_0\mu_{31}\rho_{31}, \tag{16}$$

式中：N_0 为原子密度；ε_0 为介质的介电常数；χ_p 为由探测场引起的介质极化率，即

$$\chi_p=\frac{N_0\mu_{31}}{\varepsilon_0E_p}\rho_{31}=\frac{N_0\mu_{31}^2}{2\hbar\varepsilon_0\gamma_{31}}\chi, \tag{17}$$

式中：χ 的计算公式为

$$\chi=\frac{\rho_{31}}{\Omega_p}\gamma_{31}。 \tag{18}$$

在慢变包络近似和稳态体制下，探测场的传播方程[14]可以写为

$$\frac{\partial E_p}{\partial z}=\mathrm{i}\frac{\pi}{\varepsilon_0\lambda_p}P_p, \tag{19}$$

式中：λ_p 为探测场波长。

利用(19)式，得到原子介质在 $z=L$ 处的传输函数为

$$T(x)=\exp[-\mathrm{Im}(\chi)L]\exp[\mathrm{iRe}(\chi)L], \tag{20}$$

式中：Im(•)为虚部；Re(•)为实部。

这里，L 以共振吸收长度 $z_0=2\hbar\varepsilon_0\lambda\gamma_{31}\div(\pi N_0\mu_{31}^2)$ 为单位。夫琅禾费衍射方程为

$$I_p(\theta)=|E_p^1(\theta)|^2\frac{\sin^2(M\pi\Lambda\sin\theta/\lambda_p)}{M^2\sin^2(\pi\Lambda\sin\theta/\lambda_p)}, \tag{21}$$

式中：$E_p^1(\theta)$ 为单个空间周期的夫琅禾费衍射，$E_p^1(\theta)=\int_0^1T(x)\exp(-2\pi\mathrm{i}\Lambda x\sin\theta/\lambda_p)\mathrm{d}x$，其中 M 为被探测场照射到的衍射单元数；θ 为探测场相对于 z 方向的衍射角。

3 结果与讨论

本文假设 $\gamma_{31}=\gamma_{32}=\gamma_{41}=\gamma_{42}=\gamma$，$\gamma_{43}=2\gamma$，$\Gamma_{31}=\Gamma_{32}=\Gamma_{41}=\Gamma_{42}=\gamma$，$\Gamma_{21}=\Gamma_{43}=0$。图 2(a)所示为探测场的传输函数 $T(x)$ 随 x 的变化，传输函数的相位 $\varphi=\mathrm{Re}(\chi)L$。可以看到，传输函数的振幅调制和相位调制在 x 方向上周期性地变化。调制场驱动跃迁 $|1\rangle\leftrightarrow|4\rangle$，振幅的调制幅度增大，调制幅度在 1.0～2.6 之间振荡，探测场强度增加。加入的相位调制对传输函数有很大的调制作用，传输函数的最大相位可以到达 0.93π，这使得探测场的一阶衍射效率有了很大提高。图 2(b)所示为探测场衍射强度随 $\sin\theta$ 的变化。当没有相位调制、只有振幅调制时，NRGG 的零阶衍射光强度被放大为探测场强度的 4 倍，如图 2(c)所示，此时一阶衍射光强度约为探测场强度的 20%，这表明振幅调制将光主要衍射到零阶方向。当同时考虑相位和振幅调制时，更多的能量转移到一阶和二阶衍射方向，如图 2(b)所示。这说明相位调制的存在使得探测场能量由零阶向高阶方向分散。当选取合适的参数时，NRGG 的零阶衍射光强度被放大为探测场强度的 2 倍，如图 2(c)所示，此时一阶衍射光强度约为探测场强度的 95%。当振幅调制和相位调制同时存在时，EIPG 的零阶和一阶衍射效率分别只有 21%和 30%。可以看到，NRGG 的衍射效率远高于 EIPG 和理想的正弦相位光栅的衍射效率[30]。因此，NRGG 能更好地放大探测场的能量并且显著提高高阶衍射效率。

首先讨论探测场增益的来源。图 3(a)所示为由探测场引起的介质极化率的虚部随调制场拉比频率的变化。当调制场强度较低时，极化率的虚部为正，这意味着原子介质表现为对探测场能量的吸收，而且吸收系数随调制场强度的增大而减小。当调制

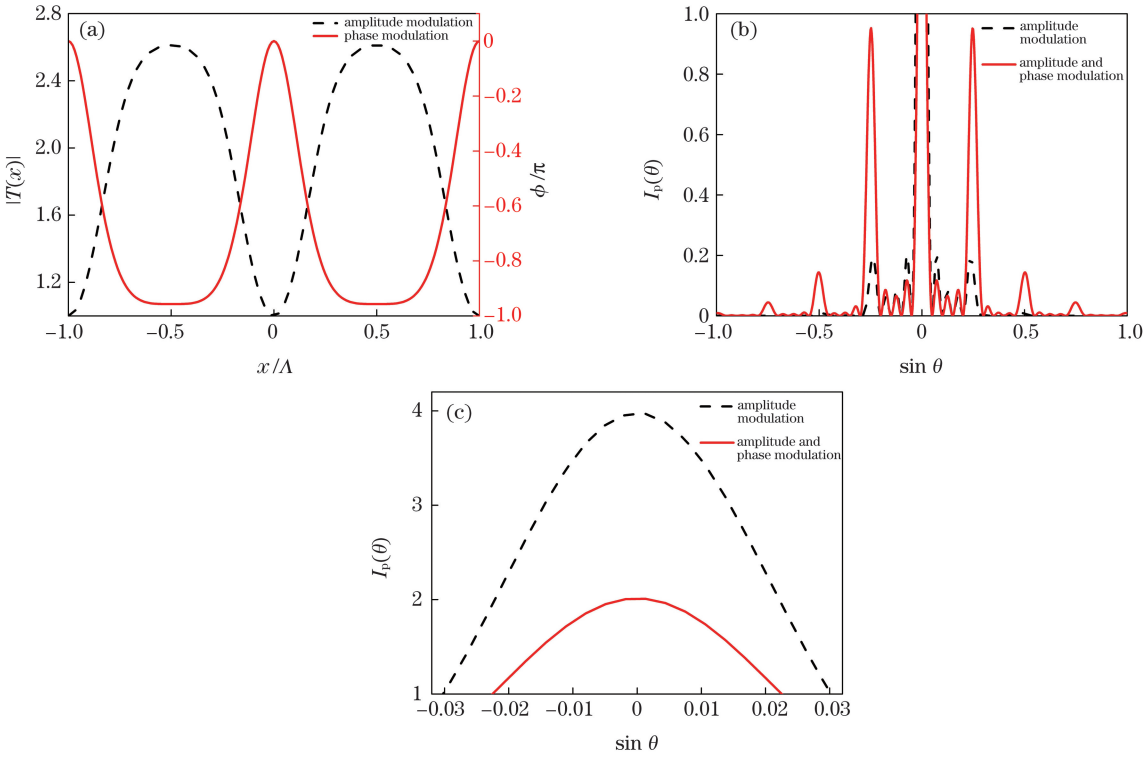

图 2 当 $\Delta_c=0$，$\Delta_m=0.68\gamma$，$\Delta_p=-0.05\gamma$，$\Omega_c=0.27\gamma$，$\Omega_m=0.35\gamma$，$L=140z_0$ 时探测场的传输函数及相应的衍射强度。(a)探测场传输函数的振幅和相位随 x 的变化；(b)不同相位调制条件下衍射强度随 sin θ 的变化；(c) 图 2(b)中零阶衍射强度大于 1.0 的部分

Fig. 2 Transmission function and corresponding diffraction intensity of probe field when $\Delta_c=0$, $\Delta_m=0.68\gamma$, $\Delta_p=-0.05\gamma$, $\Omega_c=0.27\gamma$, $\Omega_m=0.35\gamma$, and $L=140z_0$. (a) Amplitude and phase of transmission function of probe field versus x; (b) diffraction intensity versus sin θ under different phase modulation conditions; (c) part with zeroth-order diffraction intensity greater than 1.0 in Fig. 2(b)

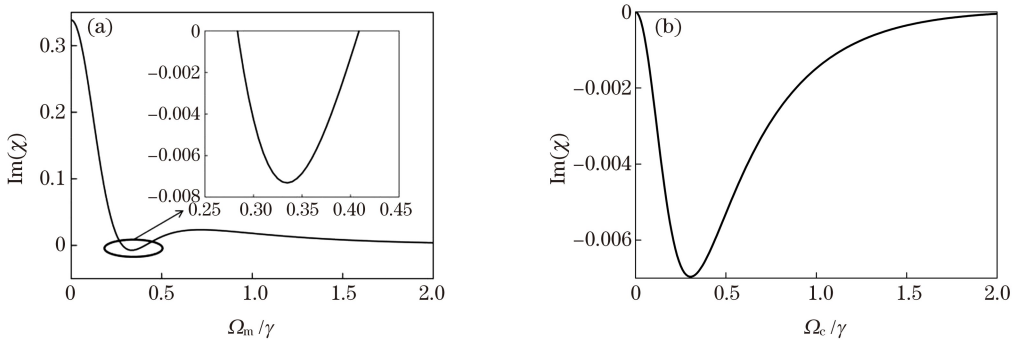

图 3 当 $\Delta_c=0$，$\Delta_m=0.68\gamma$，$\Delta_p=-0.05\gamma$，$L=140z_0$ 时 Im(χ)随调制场拉比频率和耦合场拉比频率的变化。(a) Im(χ)随调制场拉比频率的变化；(b) Im(χ)随耦合场拉比频率的变化

Fig. 3 Im (χ) versus Rabi frequencies of modulation field and coupling field when $\Delta_c=0$, $\Delta_m=0.68\gamma$, $\Delta_p=-0.05\gamma$, and $L=140z_0$. (a) Im (χ) versus Rabi frequency of modulation field; (b) Im (χ) versus Rabi frequency of coupling field

场的拉比频率为 0.28γ 时，原子介质对探测场的吸收为 0。当 Ω_m 为 $0.28\gamma\sim0.41\gamma$ 时，极化率的虚部小于 0，此时原子介质由吸收介质转变为增益介质。当调制场的拉比频率为 0.34γ 时，极化率的虚部达到最小，即探测场增益最大。随着调制场强度的继续增大，极化率的虚部也增大，此时增益减小。当调制场为 0.41γ 时，原子介质对探测场的吸收再次为 0。当 Ω_m 大于 0.41γ 时，曲线始终在 0 以上，表明探测场不再产生增益，原子介质再次转变为吸收介质。图 3(b)所示为介质极化率的虚部随耦合场拉比频率的改变。曲线总是在 0 以下，这表明随着 Ω_c 的增加，探测场始终会产生增益，且曲线的最低点代表介质的最大增益。探测场之所以始终产生增益，是因为此时 Ω_m 的取值为 $0.28\gamma\sim0.37\gamma$。如果 Ω_m

小于 0.28γ，无论耦合场取值有多大，探测场都不会有增益产生；如果 Ω_m 大于 0.37γ，只有当耦合场取一些合适的值时，探测场才有增益产生。也就是说，调制场的取值在一定范围内时探测场才会存在增益。图 3 表明调制场和耦合场的拉比频率都与探测场的增益有关，而调制场对探测场能量的放大作用更加显著。通过合理调节调制场和耦合场的强度，可以更好地放大探测场的能量。

图 4(a)、(b)、(c)分别为探测场的一阶、二阶和三阶衍射强度与 Ω_c 和 Ω_m 的关系。可以看出，当调制场和耦合场的拉比频率分别为 0.35γ 和 0.27γ 时，一阶衍射效率可达 95%左右；当调制场和耦合场的拉比频率分别为 0.36γ 和 0.55γ 时，二阶衍射效率可达 45%左右；当 Ω_m 和 Ω_c 的值分别为 0.36γ 和 0.76γ 时，三阶衍射效率可达 25%左右。此外，一阶、二阶和三阶最大衍射效率对应的 Ω_c 值分别为 0.27γ、0.55γ 和 0.76γ，说明衍射阶数越高，Ω_c 的值越大，而 Ω_m 的值基本保持不变。因此，衍射阶数主要由 Ω_c 决定，而 Ω_m 则能提高衍射的最大值。相位调制可以使探测场的能量由零阶向高阶方向转移，因此认为 Ω_c 对相位调制起着重要作用，而 Ω_m 的作用相对较小。

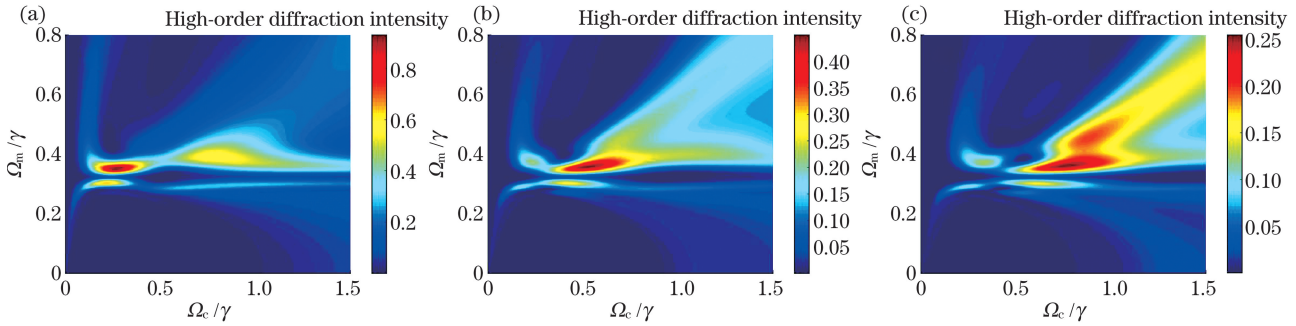

图 4　当 $\Delta_c=0$，$\Delta_m=0.68\gamma$，$\Delta_p=-0.05\gamma$，$L=140z_0$ 时高阶衍射强度随 Ω_c 和 Ω_m 的变化。(a)一阶衍射强度；(b)二阶衍射强度；(c)三阶衍射强度

Fig. 4　High-order diffraction intensity versus Ω_c and Ω_m when $\Delta_c=0$, $\Delta_m=0.68\gamma$, $\Delta_p=-0.05\gamma$, and $L=140z_0$. (a) First-order diffraction intensity; (b) second-order diffraction intensity; (c) third-order diffraction intensity

图 5(a)、(b)、(c)分别为探测场的一阶、二阶和三阶衍射强度随 Δ_p 和 Δ_m 的变化。可以看出，当探测场和调制场的失谐值分别约为 −0.058γ 和 0.78γ(或 0.058γ 和 −0.78γ)时，一阶衍射效率可达 95%左右，远远高于理想的正弦光栅的一阶衍射极限(34%)；当探测场和调制场的失谐值分别约为 −0.05γ 和0.98γ(或 0.05γ 和 −0.98γ)时，二阶衍射效率可达 24%左右；当探测场和调制场的失谐值分别为 −0.06γ 和 0.83γ(或 0.06γ 和 −0.83γ)时，三阶衍射效率可达 16%左右。因此，在探测场和调制场的失谐值很小的情况下，可获得很高的高阶衍射效率。

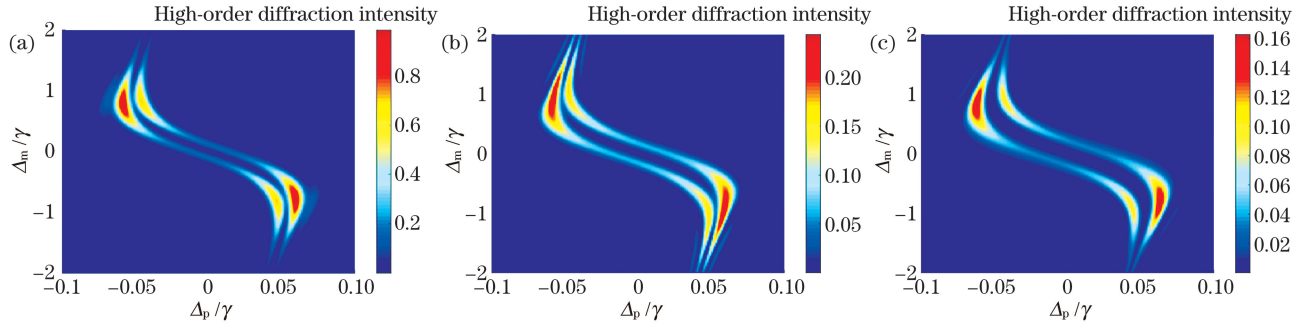

图 5　当 $\Delta_c=0$，$\Omega_c=0.27\gamma$，$\Omega_m=0.33\gamma$，$L=140z_0$ 时高阶衍射强度随 Δ_p 和 Δ_m 的变化。(a)一阶衍射强度；(b)二阶衍射强度；(c)三阶衍射强度

Fig. 5　High-order diffraction intensity versus Δ_p and Δ_m when $\Delta_c=0$, $\Omega_c=0.27\gamma$, $\Omega_m=0.33\gamma$, and $L=140z_0$. (a) First-order diffraction intensity; (b) second-order diffraction intensity; (c) third-order diffraction intensity

探测场的衍射强度随光与原子相互作用长度的变化如图 6 所示。随着相互作用长度的增加，探测场的增益提高，交叉相位调制幅度增大，因此 NRGG 衍射效率增大，且衍射效率的峰值逐渐向右偏移。最初调制场的拉比频率较小时，衍射效率几乎为 0。但当调制场的拉比频率超过一定值时，衍

射效率急剧增加，而且四条曲线的变化趋势基本相同。这说明在 NRGG 中，对于探测场的一阶衍射光，调制场强度存在阈值。例如，当 Ω_m 小于 0.26γ 时，衍射效率几乎为 0，超过 0.26γ 时，衍射效率急剧增加；当 Ω_m 的值为 0.35γ 时，一阶衍射效率达到最大，之后随着 Ω_m 的增大而逐渐减小。通过研究还发现，该阈值现象不仅在一阶衍射光中存在，在高阶光中也同样存在。例如，在相同条件下，二阶和三阶衍射光的阈值分别是 0.28γ 和 0.32γ。此结论可以被应用于全光开关和全光调制[31]中。调整的最佳结果表明，合适的调制场和耦合场的拉比频率、失谐值及光与原子相互作用的长度是得到高阶衍射效率的必要条件。

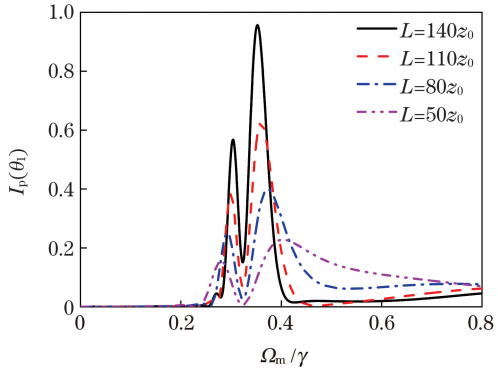

图 6 当 $\sin\theta_1=0.25$，$\Delta_c=0$，$\Delta_m=0.68\gamma$，$\Delta_p=-0.05\gamma$，$\Omega_c=0.27\gamma$，$L=140z_0$ 时不同的 L 下探测场的一阶衍射强度随 Ω_m 的变化

Fig. 6 First-order diffraction intensity versus Ω_m for different L when $\sin\theta_1=0.25$, $\Delta_c=0$, $\Delta_m=0.68\gamma$, $\Delta_p=-0.05\gamma$, $\Omega_c=0.27\gamma$, and $L=140z_0$

4 结 论

在 N 型四能级原子系统中对 NRGG 进行了理论研究。结果表明，当只有振幅调制时，在调制场和耦合场的共同作用下，探测场的能量被放大 4 倍，并且主要集中在零阶衍射方向。在加入相位调制后，耦合场对衍射光的分布起着重要作用，更多的能量转移到了高阶衍射方向。在此过程中，对于一阶、二阶和三阶衍射光来说，调制场强度存在阈值，分别为 0.26γ、0.28γ 和 0.32γ。当调制场的强度小于阈值时，几乎没有衍射光，当调制场的强度大于阈值时，各阶衍射光的强度都会急剧增加。此外，还研究了影响探测场高阶衍射效率的其他因素。通过调整相关参数，得到了增益高、衍射能力强和阈值可控的光栅，该光栅在全光开关、全光路由和全光逻辑门等新型光子器件中有广阔的应用前景。

参 考 文 献

[1] Boller K J, Imamoğlu A, Harris S E. Observation of electromagnetically induced transparency [J]. Physical Review Letters, 1991, 66(20): 2593-2596.

[2] Harris S E. Lasers without inversion: interference of lifetime-broadened resonances [J]. Physical Review Letters, 1989, 62(9): 1033-1036.

[3] Fan X J, Zhang J L, Li P, et al. Open ladder-type three level noninversion lasing system [J]. Chinese Journal of Lasers, 2002, 29(4): 327-331.
樊锡君, 张郡亮, 李萍, 等. 开放的 ladder 型三能级无粒子数反转激光系统[J]. 中国激光, 2002, 29(4): 327-331.

[4] Ling H Y. Theoretical investigation of phenomena in the closed Raman-driven four-level symmetrical model[J]. Physical Review A, 1994, 49(4): 2827-2838.

[5] Kang H, Zhu Y F. Observation of large Kerr nonlinearity at low light intensities [J]. Physical Review Letters, 2003, 91(9): 093601.

[6] Li J H, Yang W X, Peng J C. Continuous-wave four-wave mixing with linear growth based on electromagnetically dual induced transparency [J]. Chinese Optics Letters, 2004, 2(7): 418-420.

[7] Firstenberg O, Adams C S, Hofferberth S. Nonlinear quantum optics mediated by Rydberg interactions [J]. Journal of Physics B: Atomic, Molecular and Optical Physics, 2016, 49(15): 152003.

[8] Dong Y B, Wang H H, Gao J R, et al. Quantum coherence effects in quasi-degenerate two-level atomic systems [J]. Physical Review A, 2006, 74(6): 063810.

[9] Dong Y B, Zhang J X, Wang H H, et al. Observation of the widening and shifting of EIT windows in a quasi-degenerate two-level atomic system[J]. Journal of Physics B: Atomic, Molecular and Optical Physics, 2006, 39(17): 3447-3455.

[10] Bajcsy M, Zibrov A S, Lukin M D. Stationary pulses of light in an atomic medium[J]. Nature, 2003, 426(6967): 638-641.

[11] Heinze G, Hubrich C, Halfmann T. Stopped light and image storage by electromagnetically induced transparency up to the regime of one minute [J]. Physical Review Letters, 2013, 111(3): 033601.

[12] Baur S, Tiarks D, Rempe G, et al. Single-photon switch based on rydberg blockade [J]. Physical Review Letters, 2014, 112(7): 073901.

[13] Murray C R, Gorshkov A V, Pohl T. Many-body

decoherence dynamics and optimized operation of a single-photon switch[J]. New Journal of Physics, 2016, 18(9): 092001.

[14] Ling H Y, Li Y Q, Xiao M. Electromagnetically induced grating: homogeneously broadened medium [J]. Physical Review A, 1998, 57(2): 1338-1344.

[15] Xiao Z H, Shin S G, Kim K. An electromagnetically induced grating by microwave modulation[J]. Journal of Physics B: Atomic, Molecular and Optical Physics, 2010, 43(16): 161004.

[16] Bozorgzadeh F, Sahrai M, Khoshsima H. Controlling the electromagnetically induced grating via spontaneously generated coherence [J]. The European Physical Journal D, 2016, 70(9): 191.

[17] Dong Y B, Zhou Z Y, Li J Y, et al. Electromagnetically induced grating effect in room-temperature atomic system[J]. Chinese Journal of Lasers, 2017, 44(9): 0912002.
董雅宾, 周志英, 李俊燕, 等. 室温原子系统中的电磁感应光栅效应[J]. 中国激光, 2017, 44(9): 0912002.

[18] Dong Y B, Li J Y, Zhou Z Y. Electromagnetically induced grating in a thermal N-type four-level atomic system [J]. Chinese Physics B, 2017, 26(1): 014202.

[19] Tabosa J W R, Lezama A, Cardoso G C. Transient Bragg diffraction by a transferred population grating: application for cold atoms velocimetry [J]. Optics Communications, 1999, 165(1/2/3): 59-64.

[20] Brown A W, Xiao M. Frequency detuning and power dependence of reflection from an electromagnetically induced absorption grating [J]. Journal of Modern Optics, 2005, 52(16): 2365-2371.

[21] Brown A W, Xiao M. All-optical switching and routing based on an electromagnetically induced absorption grating[J]. Optics Letters, 2005, 30(7): 699-701.

[22] Sheng J T, Yang X H, Khadka U, et al. All-optical switching in an N-type four-level atom-cavity system [J]. Optics Express, 2011, 19(18): 17059.

[23] Dawes A M C. All-optical switching in rubidium vapor[J]. Science, 2005, 308(5722): 672-674.

[24] Artoni M, La Rocca G C. Optically tunable photonic stop bands in homogeneous absorbing media [J]. Physical Review Letters, 2006, 96(7): 073905.

[25] Hansen K R, Mølmer K. Trapping of light pulses in ensembles of stationary Λ atoms[J]. Physical Review A, 2007, 75(5): 053802.

[26] de Guise H, Tan S H, Poulin I P, et al. Coincidence landscapes for three-channel linear optical networks [J]. Physical Review A, 2014, 89(6):063819.

[27] de Araujo L E E. Electromagnetically induced phase grating[J]. Optics Letters, 2010, 35(7): 977-979.

[28] Sahrai M, Bozorgzadeh F, Khoshsima H. Phase control of electromagnetically induced grating in a four-level atomic system [J]. Optical and Quantum Electronics, 2016, 48(9): 438.

[29] Sadighi-Bonabi R, Naseri T. Theoretical investigation of electromagnetically induced phase grating in RF-driven cascade-type atomic systems[J]. Applied Optics, 2015, 54(11): 3484-3490.

[30] Goodman J W. Introduction to Fourier optics [M]. New York: McGraw-Hill, 1968.

[31] Li C F, Zang Z G. Optical switching in a nonlinear-fiber connected long-period fiber grating pair [J]. Chinese Journal of Lasers, 2008, 35(12): 1919-1923.
李淳飞, 臧志刚. 用非线性光纤连接的长周期光栅对的光开关特性[J]. 中国激光, 2008, 35(12): 1919-1923.

Nearly-Resonant Gain Grating in Atomic Media

Dong Yabin[1,2*], Pang Jialu[1], Yang Li[1], Liu Yaoyao[1]

[1] *College of Physics and Electronic Engineering, Shanxi University, Taiyuan, Shanxi* 030006, *China*;

[2] *Collaborative Innovation Center of Extreme Optics, Shanxi University, Taiyuan, Shanxi* 030006, *China*

Abstract

Objective With the increasing demand for high capacity and high speed information transmission, the transmission, storage, retrieval, transformation, and processing of optical information have become a very important research area in the field of information science. A grating is a type of optical device with a spatially-periodic structure. It has four main properties: dispersion, beam splitting, polarization, and phase matching. It is widely used in information processing, optical communication, optical storage, and other fields. However, when a grating is used in communications, it not only has a conversion efficiency and a conversion rate between optical and electrical signals,

but also has the response rate of a mechanical structure, which has large effects on the signal transmission efficiency, bandwidth, and stability. Therefore, all-optical networks based on the all-optical switching technology have become a new focus of research. In all-optical networks, information transmission, transformation, and amplification do not need light-electricity conversion, and the optical structures are simple, reconfigurable with anti-interference capability, thus the utilization rate of network resources is improved. The core device of an all-optical network based on an all-optical switch has the advantages of stability, high capacity, and ultra-high speed, and thus, it has attracted more and more attention from researchers. Therefore, the purpose of this study is to realize all-optical control based on grating characteristics. We achieve a nearly-resonant gain grating effect that can be used to control light in real-time and thus all-optical control is realized.

Methods In an N-type four-level atomic system, the analytical expression of the polarization rate of the probe field was first calculated by the density matrix method under the steady-state condition based on the perturbation theory. Then, the propagation equation of the probe field was obtained using Maxwell′s equations. From the analytical solution, the related factors affecting the diffraction efficiency of the probe field were analyzed, mainly including the Rabi frequencies and detunings of the modulation and coupling fields. In addition, it was seen that the transfer function of the interaction length between light and atoms also influenced the diffraction efficiency. We focused on the amplification and diffraction capacity of the probe field and generated the transmission functional curve of the probe field. The changes in diffraction intensity with Rabi frequencies, detunings of the modulation and coupling fields, and interaction length between light and atoms were also considered. A nearly-resonant gain grating with high gain and a strong diffraction ability was realized by identifying and adjusting the relevant parameters appropriately.

Results and Discussions A nearly-resonant gain grating effect is studied in an N-type four-level coherent atomic structure. The grating can not only amplify the light information, but can also actively control the light field in real-time and realize the modulation of the amplitude and phase at the same time to achieve all-optical control. When the coupling field is resonant and the probe and modulation fields are near resonance, they can regulate the gain and phase of the probe field so that the energy of the probe field is amplified and the high-order diffraction efficiency of the probe field can be significantly improved [**Fig. 2(b)**]. It is seen that the diffraction efficiency of the nearly-resonant gain grating goes beyond the theoretical limit of an ideal sinusoidal phase grating, and its diffraction efficiency is nearly three times that of a sinusoidal phase grating. In addition, during the change in the Rabi frequency of the modulation field, the atomic medium can continuously transform between the absorption and gain media [**Fig. 3(a)**]. Moreover, the modulation field has a threshold for the diffracted light during this process. When the intensity of the modulation field is less than the threshold, there is almost no diffracted light. When the intensity of the modulation field is greater than the threshold, the intensity of the each order diffracted light increases sharply (**Fig. 6**).

Conclusions We theoretically study a nearly-resonant gain grating in an N-type four-level atomic system. The results show that the energy of the probe field is amplified by four times under the combined action of the modulation and coupling fields when there is only amplitude modulation, and this is mainly concentrated in the zeroth-order diffraction direction. With the introduction of phase modulation, the coupling field plays an important role in the distribution of diffracted light, and more energy is distributed along the higher-order diffraction direction. In this process, for the first-order, second-order, and third-order diffracted light, there are thresholds for the modulation field, which are 0.28γ, 0.26γ, and 0.32γ, respectively. When the intensity of the modulation field is less than the threshold, there is almost no diffracted light, and when the intensity of the modulation field is above the threshold, the intensity of each order diffracted light increases dramatically. In addition, other factors affecting the high-order diffraction efficiency of the probe field are also studied. By adjusting the relevant parameters, a grating with high gain, strong diffraction capacity, and controllable threshold is obtained, which has broad applications in new photonic devices such as all-optical switches, all-optical routes, and all-optical logic gates.

Key words quantum optics; electromagnetically induced grating; light gain; diffraction efficiency

OCIS codes 270.1670; 190.2055; 230.1950